Biochemical Journal (2020) **477** 2735–2754
https://doi.org/10.1042/BCJ20200433

PORTLAND PRESS

Research Article

MAPK-interacting kinase 2 (MNK2) regulates adipocyte metabolism independently of its catalytic activity

James E. Merrett[1,2], Jianling Xie[1], Peter J. Psaltis[1,3] and Christopher G. Proud[1,2]

[1]Lifelong Health, South Australian Health and Medical Research Institute, Adelaide, South Australia, Australia; [2]Department of Molecular and Biomedical Science, University of Adelaide, Adelaide, South Australia, Australia; [3]Adelaide Medical School, University of Adelaide, Adelaide, South Australia, Australia

Correspondence: Christopher Proud (christopher.proud@sahmri.com)

The mitogen-activated protein kinase (MAPK)-interacting kinases (MNKs) are serine/threonine protein kinases that are activated by the ERK1/2 (extracellular regulated kinase) and p38α/β MAPK pathways. The MNKs have previously been implicated in metabolic disease and shown to mediate diet-induced obesity. In particular, knockout of MNK2 in mice protects from the weight gain induced by a high-fat diet. These and other data suggest that MNK2 regulates the expansion of adipose tissue (AT), a stable, long-term energy reserve that plays an important role in regulating whole-body energy homeostasis. Using the well-established mouse 3T3-L1 *in vitro* model of adipogenesis, the role of the MNKs in adipocyte differentiation and lipid storage was investigated. Inhibition of MNK activity using specific inhibitors failed to impair adipogenesis or lipid accumulation, suggesting that MNK activity is not required for adipocyte differentiation and does not regulate lipid storage. However, small-interfering RNA (siRNA) knock-down of MNK2 did reduce lipid accumulation and regulated the levels of two major lipogenic transcriptional regulators, ChREBP (carbohydrate response element-binding protein) and LPIN1 (Lipin-1). These factors are responsible for controlling the expression of genes for proteins involved in *de novo* lipogenesis and triglyceride synthesis. The knock-down of MNK2 also increased the expression of hormone-sensitive lipase which catalyses the breakdown of triglyceride. These findings identify MNK2 as a regulator of adipocyte metabolism, independently of its catalytic activity, and reveal some of the mechanisms by which MNK2 drives AT expansion. The development of an MNK2-targeted therapy may, therefore, be a useful intervention for reducing weight caused by excessive nutrient intake.

Introduction

In animals, highly integrated systems have evolved to promote storage during periods of energy abundance and conversely to mobilise stores during periods of energy deprivation and demand [1]. Excessive nutrient intake relative to expenditure produces a metabolic state that promotes energy storage; in the context of adipose tissue (AT), this results in adipocyte hyperplasia and hypertrophy [2]; hyperplasia involves recruitment of stem cells and their differentiation to the adipocyte lineage (adipogenesis), whereas hypertrophy involves the expansion of existing adipocyte triglyceride (TAG) stores. Given AT is fundamental for regulating whole-body energy homeostasis, it is not surprising that dysregulation or perturbation of adipose function can cause disease (reviewed in [3]). Excess or dysregulated AT expansion leads to weight gain and largely underpins the development of many chronic disorders including cardiovascular disease, hypertension and type-2 diabetes. Understanding the pathways that regulate adipocyte hypertrophy and hyperplasia is, therefore, of paramount importance.

Received: 29 May 2020
Revised: 9 July 2020
Accepted: 10 July 2020

Accepted Manuscript online: 10 July 2020
Version of Record published: 31 July 2020

PORTLAND PRESS

Biochemical Journal (2020) **477** 2735–2754
https://doi.org/10.1042/BCJ20200433

Established pre-adipocyte cell models have been indispensable for the study and identification of key transcription factors that regulate adipogenesis: 3T3-L1 pre-adipocytes are the most widely used model as they faithfully recapitulate the events that occur during *in vivo* adipogenesis [4]. Established protocols have been developed to initiate the differentiation of pre-adipocytes; inducers that activate the insulin [5], glucocorticoid and cyclic adenosine monophosphate (cAMP)-signalling pathways [4,6,7] initiate a phase of early transcription, which is followed by synchronous entry into the cell cycle and several rounds of mitosis. Upon exit from the cell cycle, cells lose their fibroblastic morphology, accumulate TAG and acquire the metabolic features and appearance of adipocytes [5,8]. TAG accumulation is closely correlated with an increased rate of *de novo* lipogenesis (DNL) and a co-ordinate rise in expression of the enzymes of fatty acid (FA) and TAG biosynthesis [9].

The program of adipogenesis involves the co-ordinated and temporal expression of several key transcriptional regulators, namely CCAAT/enhancer-binding protein (C/EBP) α, β and δ and peroxisome proliferator-activated receptor-γ (PPARγ) [1]. PPARγ and C/EBPα function as the key transcriptional regulators of adipogenesis. These two factors induce the expression of each other [10], whilst binding sites for these proteins are strongly enriched in the vicinity of genes induced in adipogenesis and in FA and glucose metabolism [11].

We previously showed that mice in which the gene encoding mitogen-activated protein kinase (MAPK)-interacting kinase 2 (MNK2) had been knocked out (MNK2-KO) exhibit protection from high-fat diet (HFD) induced obesity [12]. MNK2-KO mice have fewer but larger adipocytes which do not increase further in size on a HFD. Metabolic phenotyping indicated there is no reduction in food intake to account for the decreased weight of MNK2-KO mice (unpublished data). MNK2 is the predominant isoform in mature adipocytes and considerably induced during adipogenesis [12,13]. Furthermore, inhibiting MNK activity substantially inhibits lipid accumulation and the expression of key adipogenic genes [12]. MNK2 is, therefore, hypothesised to regulate the development of new adipocytes or indeed metabolism.

In humans and mice, there are two MNK proteins, MNK1 and MNK2, which are encoded on separate genes, *Mknk1* and *Mknk2*, respectively. The kinases exhibit similarity in their primary sequence (78% homology) and contain similar structural motifs: an N-terminal basic amino acid region that mediates localisation, a catalytic kinase domain; and an MAPK-binding domain in their carboxy-termini [14,15]. The MNKs are activated by phosphorylation, as catalysed by extracellular regulated kinase (ERK) or p38 MAPK (reviewed, [16]). MNK1 binds both ERK and p38 MAPK, which strongly activate its low basal activity [17–19]. In contrast, MNK2 binds strongly only to activated ERK and this is thought to be responsible for its constitutive high basal activity, which is not further enhanced by stimuli [20,21]. MNK1/2 are responsible for phosphorylating eukaryotic initiation factor 4E (eIF4E) [22] on its only phosphorylation site, Ser209 [23], which is the only *in vivo* validated substrate of the MNKs [16].

The aim of this study was to investigate the role of MNK2 in adipogenesis and adipocyte metabolism, and the mechanisms involved, to help explain the phenotype of MNK2-KO mice.

Materials and methods

Cell lines

Murine 3T3-L1 embryonic fibroblasts (ATCC; CL-173) were maintained in high glucose Dulbecco's modified eagle medium (DMEM) (Invitrogen; 11995-065) supplemented with 10% foetal bovine serum (Invitrogen; 10099-141) and 1% penicillin–streptomycin (Invitrogen; 15140-122) and grown at 37°C in a humidified incubator with 5% CO_2.

Differentiation of 3T3-L1 pre-adipocytes

For adipogenesis studies, 3T3-L1 pre-adipocytes were seeded at a density of 3.5×10^4 cells/cm^2 and differentiation was induced as described earlier [12] with minor modifications. Cells were grown for 2-days after they reached confluence ('day 0') at which point the medium was replaced with growth medium freshly supplemented with 350 nM insulin, 500 µM 3-isobutyl-1-methylxanthine, 0.5 µM dexamethasone and 2 µM rosiglitazone (differentiation medium). On day 3, the medium was replaced with growth medium supplemented with 350 nM insulin (maintenance medium). The maintenance medium was replenished every 3-days until the cells were utilised for experimentation or the end-point of differentiation was reached (day 9). When assaying the effect of MNK inhibitors on adipocyte differentiation, compounds were added at the time of cell seeding (pre-treatment) and supplemented at each change of medium, unless indicated otherwise. The MNK inhibitor

Biochemical Journal (2020) 477 2735–2754
https://doi.org/10.1042/BCJ20200433

Table 1. SilencerSelect siRNA assays

siRNA	Catalog. no.	Assay no.
Mknk1 #1	4 390 771	s69877
Mknk1 #2		s69878
Mknk2 #1		s69880
Mknk2 #2		s69881
Clk1		s64055
Clk4		s64060
Gapdh	4 390 849	
Scrambled	4 390 844	

eFT508 [24] was purchased from Jomar Life Research. MNK-I1 was kindly provided by Professor Jiang Tao School of Medicine and Pharmacy, Ocean University of China, 5 Yushan Road, Qingdao, China.

siRNA knock-down

SilencerSelect siRNA (ThermoFisher) were used to silence protein expression in 3T3-L1 cells (Table 1). siRNA was transfected using Lipofectamine RNAiMAX Transfection Reagent (Invitrogen; 13778150) in a 1 : 3 ratio, according to the manufacturer's instructions, except that reagent and siRNA dilutions were made in serum and antibiotic-free DMEM (Invitrogen; 11995-065), not Opti-MEM. Where more than one siRNA was directed against a single gene, the molar ratio of each siRNA was proportioned so that the total molar amount (25 pmol) remained the same. When assaying the effect of siRNA-mediated knock-down on adipocyte differentiation, cells were transfected 24 h after seeding, then re-transfected 3-days post-induction.

Oil red O (ORO) staining

A 0.35% (w/v) solution of ORO (Sigma–Aldrich) in isopropanol was prepared and used to stain differentiated adipocytes, according to the manufacturer's recommendations. Stained cells were imaged on a ZEISS Axio Vert A1 inverted microscope (ZEISS) using a 5X objective lens; six representative images were captured per well and quantified using a macro script in Image J (NIH). Following imaging, the amount of lipid staining (per well) was assayed semi-quantitatively by eluting ORO in 100% isopropanol for 5 min and measuring the absorbance at 490 nm.

Metabolic assays

For all metabolic assays, 3T3-L1 cells were seeded in 96-well assay plates, transfected with or without siRNA as appropriate, and subjected to adipogenic differentiation, as described above.

Glucose uptake was measured using the Glucose Uptake-Glo Assay (Promega; J1341) and following the manufacturer's recommendations. Briefly, cells were starved of serum prior to the assay by incubation in serum-free DMEM (SF-DMEM) overnight. On the day of the assay (day 9), cells were treated with SF-DMEM without glucose (Invitrogen; 11966-025, with 1 mM sodium pyruvate), supplemented with insulin (0.01, 0.1, 1, 10 or 100 nM) for 1 h. Cells were then treated with 1 mM 2-deoxyglucose (2DG), diluted in PBS for 10 min at room temperature. Luminescence, corresponding to the amount of 2-DG uptake, was recorded using the GloMax Discoverer (Promega) with 0.3–1 s integration.

Lipolysis was measured using the Lipolysis Assay Kit (Abcam; ab185433). On day 9, cells were washed twice with Lipolysis Wash Buffer, then stimulated with or without 100 nM isoproterenol (in sterile water) for 3 h. The assay was conducted according to the manufacturer's recommendations. Absorbance at 570 nm was measured using the GloMax Discoverer (Promega) and glycerol concentration was determined using a standard curve.

Lactate levels were assayed using the L-Lactate Assay Kit (Abcam; ab65330) in medium collected from differentiating adipocytes on day 6. Medium samples were first diluted 1 : 1000 in assay buffer, then 2 µl of this dilution was assayed in duplicate in black polystyrene microplates (Corning; CLS3631). The assay was conducted according to the manufacturer's recommendations for a fluorometric assay. Fluorescence output (ex/em:520/

Biochemical Journal (2020) **477** 2735–2754
https://doi.org/10.1042/BCJ20200433

Table 2. TaqMan assay probes used for RT-qPCR gene expression analyses

Gene	Assay ID
Acaca	Mm01304257_m1
Acacb	Mm01204671_m1
Acly	Mm01302282_m1
Cd36	Mm00432403_m1
Chrebpa	Mm02342723_m1
Dgat1	Mm00515643_m1
Dgat2	Mm00499536_m1
Fasn	Mm0062319_m1
Hprt	Mm03024075_m1
Lipe	Mm00495349_m1
Lpin1	Mm00550511_m1
Lpl	Mm00434764_m1
Mgll	Mm0449274_m1
Nono	Mm00834875_g1
Pck1	Mm01247058_m1
Plin1	Mm00558672_m1
Pnpla2	Mm00503040_m1
Sfrp5	Mm01194236_m1
Slc2a4	Mm00436615_m1
Srebf1	Mm00550338_m1

580 nm) was measured using the GloMax Discoverer (Promega). L-Lactate concentration was determined using a standard curve and adjusted to the relevant dilution factor.

RNA isolation

RNA was routinely harvested from cells using TRI Reagent (Sigma; T9424) and cDNA synthesised using the QuantiNova Reverse Transcription Kit (Qiagen; 205413), according to the manufacturer's recommendations. Quantitative gene expression analysis was performed using TaqMan Fast Advanced MasterMix (Applied Biosystems) on a 7500 Fast Real Time PCR System (Applied Biosystems). RT-qPCR reactions were performed using pre-designed TaqMan assay probes (Table 2), whilst *Mknk1*, *Mknk2* and *Gapdh* expression analysis was performed using Fast SYBR Green Master Mix (Applied Biosystems; 4385617) with gene-specific primers (Table 3). All reactions were performed in triplicate. Relative gene expression was determined using $2^{-\Delta\Delta Ct}$, with the geometric mean of *Nono* and *Hprt* used as the internal reference.

Table 3. Primers used for RT-qPCR gene expression analyses

Gene	F Primer (5′-3′)	R Primer (5′-3′)
Gapdh	GGGTTCCTATAAATACGGACTGC	CCATTTTGTCTACGGGACGA
Mknk1	GATTCCTCTGAGACTCCAAGTTAA	ACGCTTCTTCTTCCTCCTCTT
Mknk2	CCAGTGCCAGGGACATAGG	GCCACGCATCTTCTCAAACA

Biochemical Journal (2020) 477 2735–2754
https://doi.org/10.1042/BCJ20200433

Extraction of proteins

Cell monolayers were harvested on ice in RIPA lysis buffer (50 mM Tris–HCl, pH 7.5, 150 mM NaCl, 1% (v/v) NP-40, 1% (v/v) sodium deoxycholate, 0.1% (v/v) sodium-dodecyl sulfate (SDS), 1 mM ethylenediaminetetra-acetic acid (EDTA), 50 mM β-glycerophosphate, 0.5 mM NaVO3, 0.1% (v/v) 2-mercaptoethanol and 1× protease inhibitors (Roche; 11836170001). Insoluble material was removed by centrifuging at >12 000×***g*** for 10 min at 4°C. Protein content was determined by the Bradford protein assay (Bio-Rad; 5000006) and lysates prepared to equal concentrations.

Immunoblot analyses

Cell lysates were heated at 95°C for 5 min in Laemmli Sample Buffer and then subjected to sodium-dodecyl sulfate polyacrylamide gel electrophoresis (SDS–PAGE; [25]) followed by electrophoretic transfer to 0.45 µm nitrocellulose membranes (Bio-Rad; 1620115). Membranes were blocked in PBS-0.05% Tween20 (PBST) containing 5% (w/v) skim milk powder for 60 min at room temperature. Membranes were probed with the primary antibody in PBST with 5% BSA (w/v) (Table 4) overnight at 4°C. Membranes were then washed (3 × 5 min) in PBST and incubated with fluorescently tagged secondary antibody, diluted in PBST, for 1 h. Membranes were washed again in PBST (3 × 5 min) and fluorescent signals were visualised using the Odyssey Quantitative Imaging System (LI-COR, Lincoln, NE) and quantified using Image Studio software (v5.2.5).

Table 4. Primary antibodies used for detection of proteins by Western blot. Abbreviations: M: mouse, R: Rabbit

Target	Dilution	Species	Catalog. no.	Supplier
eIF4E	1 : 1000	R	CST-9742	Cell Signaling Technology
P-eIF4E (Ser209)	1 : 1000	R	PA-44528G	ThermoFisher
rpS6	1 : 1000	M	sc-74459	Santa-Cruz
P-rpS6 (Ser240/244)	1 : 1000	R	CST-2215	Cell Signaling Technology
ERK	1 : 1000	R	CST-9102	Cell Signaling Technology
P-ERK (Thr202/Tyr204)	1 : 1000	R	CST-4370	Cell Signaling Technology
PKB	1 : 1000	R	CST-4685	Cell Signaling Technology
P-PKB (Ser473)	1 : 500	R	CST-9271	Cell Signaling Technology
4EBP1	1 : 1000	R	CST-9644	Cell Signaling Technology
P-4EBP1 (Ser65)	1 : 500	R	CST-9451	Cell Signaling Technology
ACTIN	1 : 5000	M	A2228	Sigma
GAPDH	1 : 5000	M	G8795	Sigma
C/EBPα	1 : 500	R	CST-2295	Cell Signaling Technology
C/EBPβ	1 : 500	R	sc-150	Santa-Cruz
P-C/EBPβ (Thr188)	1 : 500	R	CST-3084	Cell Signaling Technology
C/EBPδ	1 : 500	R	CST-2318	Cell Signaling Technology
PPARγ	1 : 1000	R	CST-2443	Cell Signaling Technology
GLUT4	1 : 1000	M	CST-2213	Cell Signaling Technology
PLIN1	1 : 1000	R	CST-9349	Cell Signaling Technology
LPIN1	1 : 1000	R	CST-14906	Cell Signaling Technology
FABP4	1 : 1000	R	CST-3544	Cell Signaling Technology
ATGL	1 : 1000	R	CST-2439	Cell Signaling Technology
HSL	1 : 1000	R	CST-18381	Cell Signaling Technology
FASN	1 : 1000	R	CST-3180	Cell Signaling Technology
MNK1	1 : 1000	R	CST-2195	Cell Signaling Technology

PORTLAND PRESS

Biochemical Journal (2020) **477** 2735–2754
https://doi.org/10.1042/BCJ20200433

Results and discussion

To study the individual contributions of MNK1 and MNK2 to adipocyte differentiation, siRNAs directed against *Mknk1* (si*Mknk1* #1/#2) and *Mknk2* (si*Mknk2* #1/#2) were employed. The siRNAs were assayed individually (#1/#2) or in combination (#1+#2) for their efficacy in knocking down MNK expression in 3T3-L1 pre-adipocytes. Both siRNAs directed against *Mknk1* reduced the expression of the *Mknk1* mRNA and MNK1 protein (Figure 1A,B). Both *Mknk2*-directed siRNAs decreased expression of the *Mknk2* mRNA, individually and in combination, as expected (Figure 1C). Interestingly, knock-down of *Mknk2* tended to increase the levels of the *Mknk1* mRNA (Figure 1A), hinting at possible cross-talk/feedback regulation. This may be a compensatory response to the loss of MNK2 (the main MNK species in this cell type); however, as there is yet no published information on the transcriptional control of MNK expression, it is not clear what mechanisms might be involved. All siRNAs appeared to be isoform-specific with the exception of si*Mknk1* #2, which partially reduced *Mknk2* levels (Figure 1B). siRNA for *Gapdh* did not affect MNK expression but did very markedly decrease levels of the *Gapdh* mRNA and protein (Figure 1B,D), suggesting that the transfection/knock-down procedure was effective. As no suitable commercial MNK2 antibody is available [26,27], knock-down of MNK2 was assessed by measuring the phosphorylation of eIF4E (p-eIF4E), a readout of MNK activity. Both *Mknk2*-directed siRNAs almost completely abolished p-eIF4E; with the residual phosphorylation being attributable to MNK1 since si*Mknk1* and si*Mknk2* used in combination completely abolished p-eIF4E (Figure 1D). *Mknk1*-directed siRNAs did not markedly affect p-eIF4E levels (Figure 1B) suggesting that MNK2 is the predominant MNK isoform in these cells.

In light of this, it was important to establish the relative activities of the MNK isoforms in 3T3-L1 pre-adipocytes. Serum-starved 3T3-L1 cells, silenced for MNK1, MNK2 and MNK1/2 expression by siRNA transfection, were treated with DMSO or the phorbol ester tetradecanoylphorbol acetate (TPA), which activates ERK by stimulating an upstream kinase (protein kinase C), to monitor basal and induced levels of p-eIF4E, respectively. Under basal conditions, p-eIF4E was almost completely abolished in MNK2-, but not MNK1-knock-down cells (Figure 1E,F). The residual P-eIF4E seen in si*Mknk2* cells was likely attributable to MNK1 since it was lost when si*Mknk1* and *siMknk2* were combined (Figure 1E,F). TPA stimulation of MNK2 knock-down cells elevated p-eIF4E beyond basal levels, indicating that MNK1 activity is significantly increased in response to TPA (Figure 1E,F), consistent with the known properties of MNK1 [14,18]. However, TPA stimulation was unable to elevate p-eIF4E levels above basal in MNK1-knock-down cells, indicating that, as expected, the high basal activity of MNK2 cannot be further enhanced by stimuli (Figure 1E,F). These data suggest that MNK2 is principally responsible for maintaining basal p-eIF4E levels, whilst MNK1 is exclusively responsible for inducible p-eIF4E in 3T3-L1 pre-adipocytes. These findings are consistent with the established properties of MNK1/2 [14,17,18].

Given that MNK2 is the major isoform in mouse AT and its expression is considerably induced during adipocyte differentiation [12], MNK2 was proposed to play a role in adipogenesis. To investigate this, MNK2 expression was knocked-down in 3T3-L1 cells using si*Mknk2* (#1+#2) which were subject to adipogenic induction. As expected, si*Mknk2* transfection decreased both *Mknk2* mRNA and p-eIF4E levels, indicating the successful knock-down of MNK2 (Figure 2A,B). Notably, the expression of C/EBPβ, C/EBPδ, C/EBPα and PPARγ was not affected by the knock-down of MNK2, nor was the level of p-C/EBPβ (a pre-requisite for dimerisation and DNA binding), indicating that the DNA binding activity of C/EBPβ is not regulated by MNK2 (Figure 2B). C/EBPα and PPARγ expression was normal, as were the levels of proteins encoded by downstream target mRNAs: PLIN1, ATGL and FABP4 (except for small decreases on day 3, which recovered at later times), suggesting that MNK2 does not regulate, and is, therefore, not required for adipogenesis itself (Figure 2B).

Intriguingly, despite this, lipid accumulation was significantly reduced by the knock-down of MNK2, as quantified by ORO staining and absorbance of eluted ORO (Figure 2C–E). Since the reduced lipid content could not be directly attributed to a defect in adipogenesis (adipocyte differentiation; Figure 2B), it was apparent that MNK2 may regulate aspects of lipid metabolism in adipocytes. In terms of metabolism, a decrease in lipid accumulation may be attributable to decreased lipogenesis (lipid synthesis), increased lipolysis (lipid breakdown) or a combination of both.

LPIN1 is induced during 3T3-L1 adipogenesis and is thought to be critical for adipocyte development *in vivo* and *in vitro*, as it is required for the expression of PPARγ and C/EBPα [28,29]. LPIN1 is also responsible for converting phosphatidate to diacylglycerol (DAG), a key step in the synthesis of TAG [30,31], and acts as a transcriptional activator of genes involved in lipid metabolism [28,32]. Interestingly, LPIN1 expression was

Biochemical Journal (2020) **477** 2735–2754
https://doi.org/10.1042/BCJ20200433

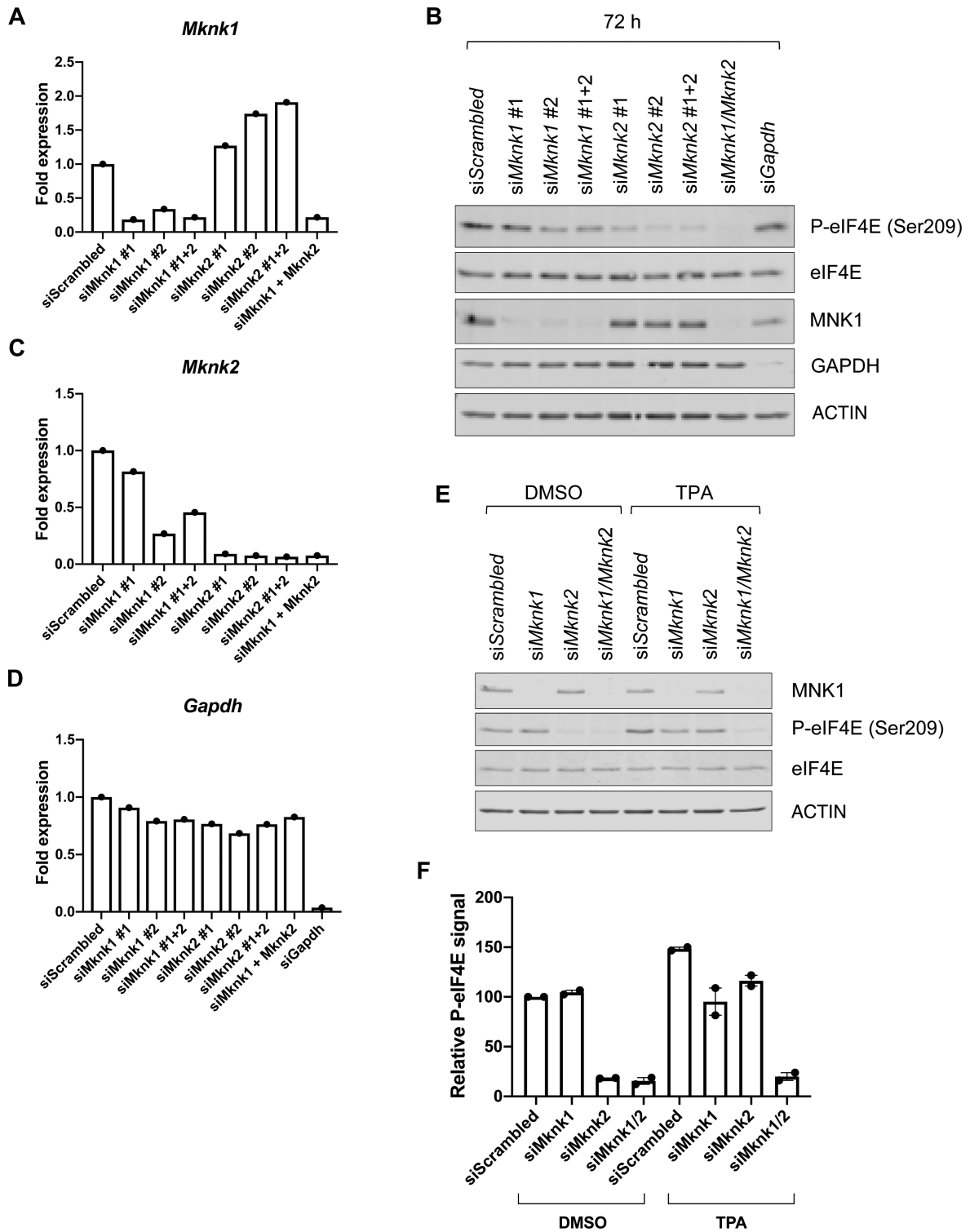

Figure 1. siRNA-mediated knock-down of MNK1 and MNK2 in 3T3-L1 cells.

3T3-L1 pre-adipocytes were transfected with siRNA individually or in combination, as indicated. After 72 h, the mRNA levels of (**A**) *Mknk1*, (**C**) *Mknk2* and (**D**) *Gapdh* were measured by RT-qPCR ($n = 1$) whilst the levels of (**B**) p-eIF4E, eIF4E, MNK1, GAPDH and ACTIN were monitored by Western blot; representative immunoblots are shown ($n = 2$). (**E**) siRNA-treated 3T3-L1 cells were serum-started overnight (16 h) and stimulated with 100 mM TPA or equivalent volume of DMSO for 15 min. The levels of MNK1, p-eIF4E, eIF4E and ACTIN were monitored by Western blot. (**F**) p-eIF4E was quantified from (**E**), relative to si*Scrambled*; data are mean ± SEM ($n = 2$); ordinary one-way ANOVA (*$P < 0.05$ **$P < 0.01$ ***$P < 0.001$).

Biochemical Journal (2020) 477 2735–2754
https://doi.org/10.1042/BCJ20200433

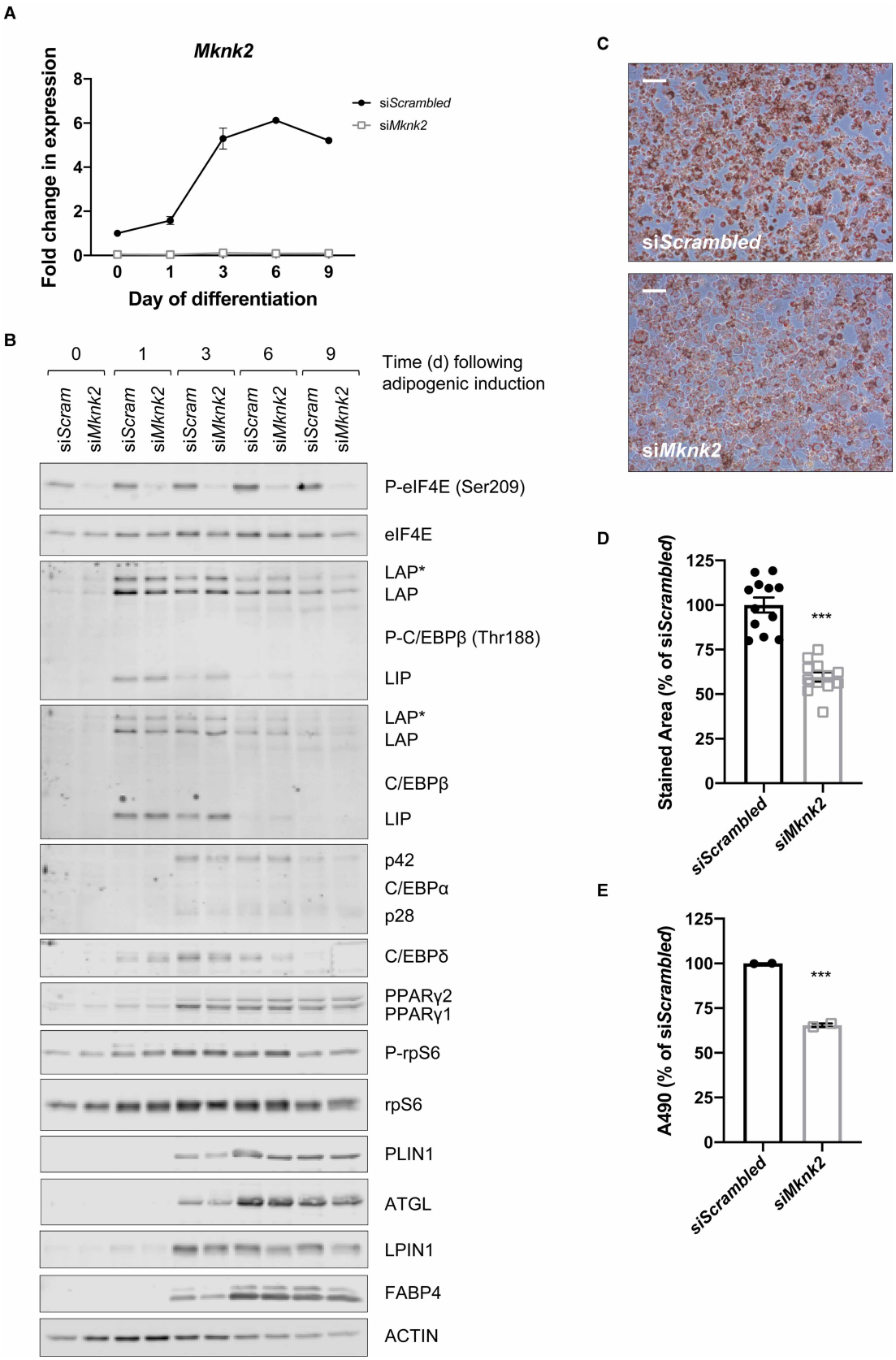

Figure 2. Effect of MNK2 knock-down on 3T3-L1 adipogenesis. Part 1 of 2

3T3-L1 pre-adipocytes were transfected with siRNA, as indicated. (**A**) The mRNA level of *Mknk2* was measured by RT-qPCR

Biochemical Journal (2020) 477 2735–2754
https://doi.org/10.1042/BCJ20200433

Figure 2. Effect of MNK2 knock-down on 3T3-L1 adipogenesis. Part 2 of 2

($n = 3$) and (**B**) protein expression monitored by Western blot using the indicated antibodies; representative immunoblots are shown ($n = 4$) (**C**) Day 9 differentiated adipocytes were stained with ORO to assess lipid accumulation; representative images are shown, scale bar 0.2 μm. (**D**) Total stained area was quantified from (**C**) or from the absorbance of eluted ORO at 490 nm (**E**); data are mean ± SEM ($n = 2$); unpaired *t*-test (*$P < 0.05$ **$P < 0.01$ ***$P < 0.001$).

reduced in MNK2 knock-down cells, most notably during terminal differentiation (Figure 2B). The mRNA for LPIN1 is alternatively spliced, thereby producing two protein isoforms designated LPIN1α and LPIN1β. These isoforms are expressed differentially and exhibit distinct functions: LPIN1α is involved in adipocyte differentiation, whereas LPIN1β has a pronounced effect on the induction of lipogenic genes [32]. Given that LPIN1β is the predominant isoform during the later stages of adipogenesis [32], MNK2 may, therefore, promote the expression of LPIN1β either through regulation of alternative splicing or selective mRNA translation.

To examine the robustness and validity of the reduced lipid phenotype, 3T3-L1 cells were treated individually with either si*Mknk2* #1 or #2. As expected, si*Mknk2* #1 and #2 each decreased p-eIF4E levels, confirming the successful knock-down of MNK2 (Supplementary Figure S1A,B). The expression of C/EBPβ, C/EBPδ, C/EBPα and PPARγ was not affected by either si*Mknk2* #1 or #2, nor was the level of p-C/EBPβ (Supplementary Figure S1A,B), as would be expected from the above data. Furthermore, the expression of downstream proteins induced during terminal differentiation (ATGL, FABP4) was also unaffected, as expected. The expression of PLIN1 (a lipid droplet protein) was partially reduced by si*Mknk2* #1 on days 3 and 6 but not by si*Mknk2* #2; it is not clear why. Notably, LPIN1 expression was reduced by both si*Mknk2* #1 and #2 and each significantly reduced lipid accumulation, although the effect was greater with si*Mknk2* #2 (∼40%) than si*Mknk2* #1 (∼30%), as quantified by ORO staining (Supplementary Figure S1C,D); this may be due to the fact that si*Mknk2* #2 decreases *Mknk2* expression more strongly than si*Mknk2* #1 (Figure 1B). Nevertheless, these findings clearly implicate MNK2 in the control of adipocyte lipid metabolism, which may reflect effects on LPIN1 expression.

To understand which aspect(s) of lipid metabolism was specifically affected by the knock-down of MNK2 and identify pathways that might be subject to its regulation, the expression of genes associated with adipocyte metabolism were assessed by RT-qPCR in differentiating 3T3-L1 pre-adipocytes in which *Mknk2* expression had been knocked down.

In DNL, ATP citrate lyase (encoded by *Acly*) catalyses the conversion of citrate to acetyl-CoA which is then converted by acetyl-CoA carboxylase 1 (*Acaca*) to malonyl-CoA, the essential precursor for FA synthesis, catalysed by fatty acid synthase (*Fasn*) (schematised in Supplementary Figure S2). Expression of *Acly*, *Acaca* and *Fasn*, the key enzymes of DNL, was significantly reduced by si*Mknk2* on days 6 and 9 (Figure 3A–C). This suggests that the capacity for DNL was significantly reduced by MNK2 knock-down. It should be noted that similar reductions in mRNA gene expression were observed when each of the siRNAs against *Mknk2* was used individually (see Supplementary Figure S3).

In the pathway of TAG synthesis, FAs are covalently linked to a glycerol backbone (Supplementary Figure S2); glycerol-3-phosphate (G3P) acyltransferase (GPAT) enzymes catalyse the addition of the first FA to G3P, while the second and third FAs are added by enzymes known as acyl-glycerophosphate acyltransferases (AGPATs) and diacylglycerol-acyltransferases (DGATs), respectively [33]. *Dgat1*, and particularly *Dgat2*, are highly expressed in AT and catalyse the final rate-limiting step of TAG synthesis [34,35]. The levels of *Dgat1* and *Dgat2* were significantly reduced by the knock-down of MNK2 on day 6 (Figure 3D,E). *Lpin1* levels were also significantly reduced by si*Mknk2* on day 6 (Figure 3F). As alluded to previously, LPIN1 is also a transcriptional activator of lipogenic gene expression; reduced LPIN1 expression may impair DNL in two ways: a reduction in the availability of substrate for TAG synthesis and impaired transcription of genes for enzymes of lipogenesis.

Acetyl-CoA carboxylase 2 (*Acacb*) is expressed at high levels in AT [36] and is localised to mitochondria where it regulates FA oxidation [37], since its product, malonyl-CoA, inhibits the rate-limiting enzyme of FA oxidation, carnitine palmitoyl-transferase I. *Acacb*$^{-/-}$ mice have increased rates of β-oxidation because they are unable to produce sufficient malonyl-CoA and are thus protected from diet-induced obesity [38]. In MNK2 knock-down adipocytes, *Acacb* expression was significantly reduced on day 9 (Figure 3G), suggesting the rate of FA oxidation may be increased, which could contribute to their reduced lipid content. This may have broader implications in other FA-oxidising tissues, such as the heart and muscle, and may be particularly

Biochemical Journal (2020) 477 2735–2754
https://doi.org/10.1042/BCJ20200433

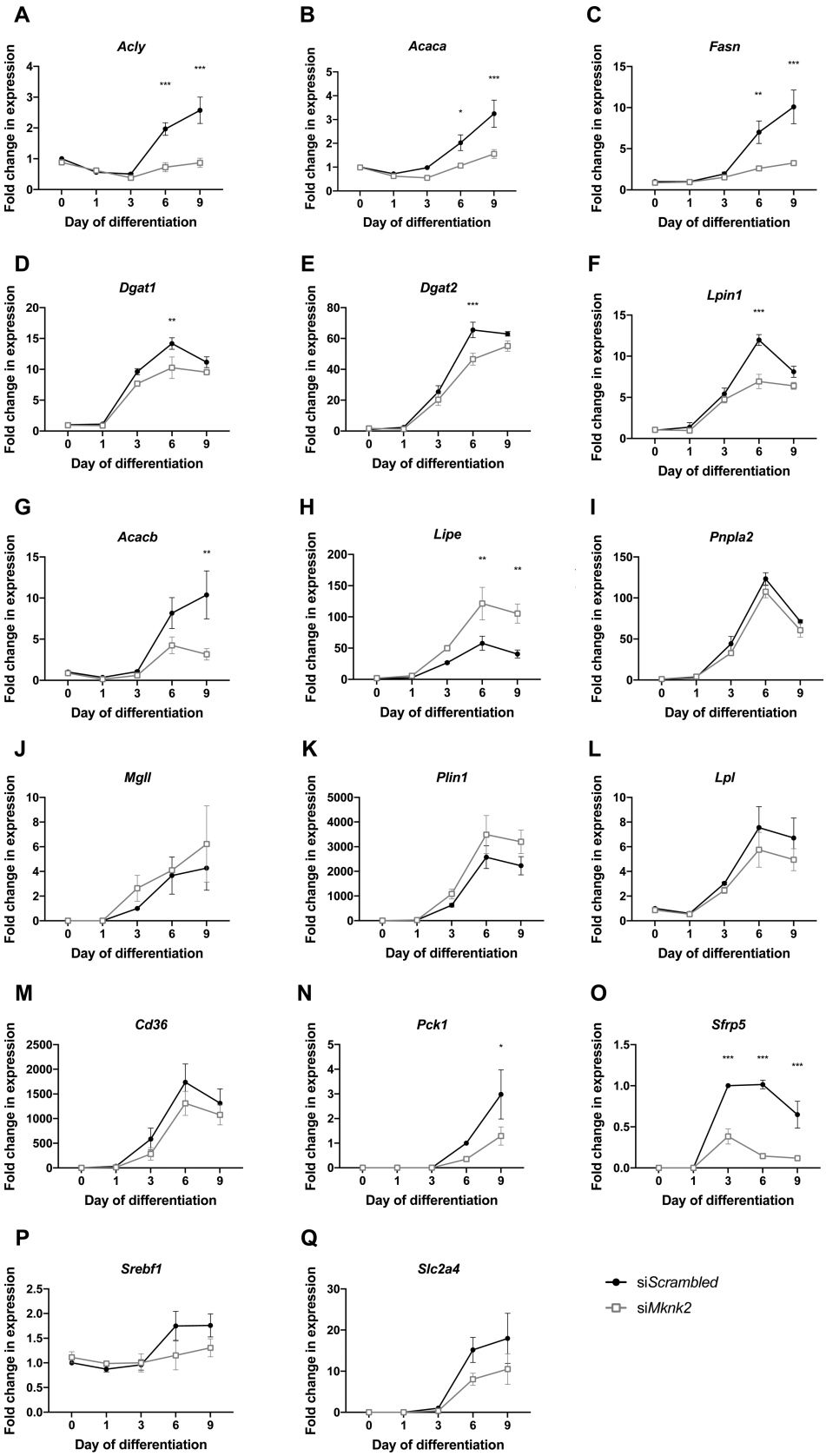

Figure 3. Effect of MNK2 knock-down on metabolic gene expression in 3T3-L1 adipocytes. Part 1 of 2

3T3-L1 pre-adipocytes were transfected with siRNA as indicated. The mRNA levels of (**A**) *Acly*, (**B**) *Acaca*, (**C**) *Fasn*, (**D**) *Dgat1*,

Biochemical Journal (2020) **477** 2735–2754
https://doi.org/10.1042/BCJ20200433

Figure 3. Effect of MNK2 knock-down on metabolic gene expression in 3T3-L1 adipocytes. Part 2 of 2
(**E**) *Dgat2*, (**F**) *Lpin1*, (**G**) *Acacb*, (**H**) *Lipe*, (**I**) *Pnpla2*, (**J**) *Mgll*, (**K**) *Plin1*, (**L**) *Lpl*, (**M**) *Cd36*, (**N**) *Pck1*, (**O**) *Sfrp5*, (**P**) *Srebf1* and (**Q**) *Slc2a4* were assessed by RT-qPCR at the indicated times. Data are mean ± SEM ($n = 3$); 2-way ANOVA (*$P < 0.05$ **$P < 0.01$ ***$P < 0.001$).

relevant for understanding the *in vivo* MNK2-KO phenotype in which mice are protected from HFD-induced weight gain [12].

Among enzymes involved in lipolytic pathways, MNK2 knock-down significantly increased the levels of hormone-sensitive lipase (HSL) (*Lipe*), the key enzyme of DAG hydrolysis (Figure 3H). Interestingly, the levels of adipocyte triglyceride lipase (ATGL) (*Pnpla2*) and monoacylglycerol lipase (*Mgll*), which catalyse the hydrolysis of TAG/DAG and MAG, respectively, were not significantly affected by the knock-down of MNK2 (Figure 3I,J).

The lipid droplet surface is complexed with one or more members of the Perilipin family of proteins which help to stabilise the droplet and regulate lipolysis [39]; PLIN1 (*Plin1*) is regarded as the major lipid droplet protein and is central to the regulation of lipolysis in adipocytes. Although lipid content was reduced in MNK2 knock-down adipocytes, *Plin1* levels were not significantly affected (Figure 3K), suggesting the expression of PLIN1, and presumably its control of lipolysis at the lipid-droplet interface, are not regulated by MNK2.

Lipoprotein lipase (*Lpl*) is expressed in the endothelium and is responsible for the breakdown of TAG in circulating chylomicrons and lipoprotein particles [40]. *Lpl* levels were not significantly affected by the knock-down of MNK2, although they did trend lower (Figure 3L). Furthermore, the level of the FA transport protein, *Cd36*, which is responsible for the uptake of exogenous FAs into adipocytes [41] was not significantly affected by MNK2 knock-down but also trended lower (Figure 3M). This suggests the uptake of exogenous FAs is unlikely to be regulated by MNK2, which is consistent with the fact that MNK2-KO mice have normal circulating levels of FAs [12].

Lipid metabolism is in a constant state of flux, where during periods of lipolysis, a considerable proportion of FAs is re-esterified back into TAG [42]. This 'recycling' of FAs is thought to be important for regulating lipid homeostasis and FA release during fasting [43]. G3P is required for the re-esterification of FA, and indeed the synthesis of TAG from lipogenic pathways. However, under conditions where lipolysis is activated, the major source of G3P, glycolysis, is markedly reduced [43]. Glycerol kinase is also expressed at a very low level in AT, and so after complete hydrolysis of TAG, very little of the glycerol backbone can be phosphorylated back to G3P. A metabolic pathway, known as glyceroneogenesis, is required for the synthesis of G3P from non-carbohydrate substrates, such as pyruvate and lactate, when glucose levels are low. Phosphoenolpyruvate carboxykinase 1 (*Pck1*) is the major enzyme regulating glyceroneogenesis [44]. The knock-down of MNK2 significantly reduced the level of *Pck1* (Figure 3N), suggesting that the availability of G3P for TAG synthesis and FA recycling may be reduced.

Secreted frizzled-related protein 5 (*Sfrp5*) antagonises Wnt signalling and has been widely implicated in adipocyte biology [45]. Multiple studies report that *Sfrp5* is highly induced with genetic or diet-induced obesity [46–48], although one study reported that *Sfrp5* is actually suppressed under these conditions [49]. In MNK2 knock-down adipocytes, *Sfrp5* levels were significantly reduced (Figure 3O). *Sfrp5* expression is one of the best a priori predictors of adiposity in mice prior to HFD exposure [46] which is consistent with the protection of MNK2-KO mice from HFD-induced weight gain [12].

Given the changes in metabolic gene expression largely affected genes in lipogenic pathways, it seemed possible that a transcription factor(s) responsible for the regulation of lipid metabolism was regulated by MNK2. Sterol regulatory element-binding protein 1 (*Srebf1*) enhances the transcriptional activity of PPARγ and thereby promotes the expression of genes involved in FA and lipid metabolism [50,51]. The level of *Srebf1* was not, however, significantly affected by the knock-down of MNK2, although it did trend lower (Figure 3P). Carbohydrate response element-binding protein (ChREBP) is a lipogenic transcription factor that is activated by carbohydrate feeding [52] and increases during adipocyte differentiation [53–55].

In the context of 3T3-L1 adipocytes, which are cultured in high-glucose medium, ChREBP is thus particularly relevant. In MNK2 knock-down adipocytes, on days 6 and 9, the level of ChREBP protein was significantly reduced as was *Chrebpa* mRNA (Figure 4A–C). Notably, three genes among our data set that are considered as targets for ChREBP [56,57], i.e. *Acly*, *Acaca* and *Fasn* were very substantially decreased by the knock-down of MNK2 (Figure 3A–C), consistent with the lower levels of ChREBP. Notably, the levels of FAS

Biochemical Journal (2020) 477 2735–2754
https://doi.org/10.1042/BCJ20200433

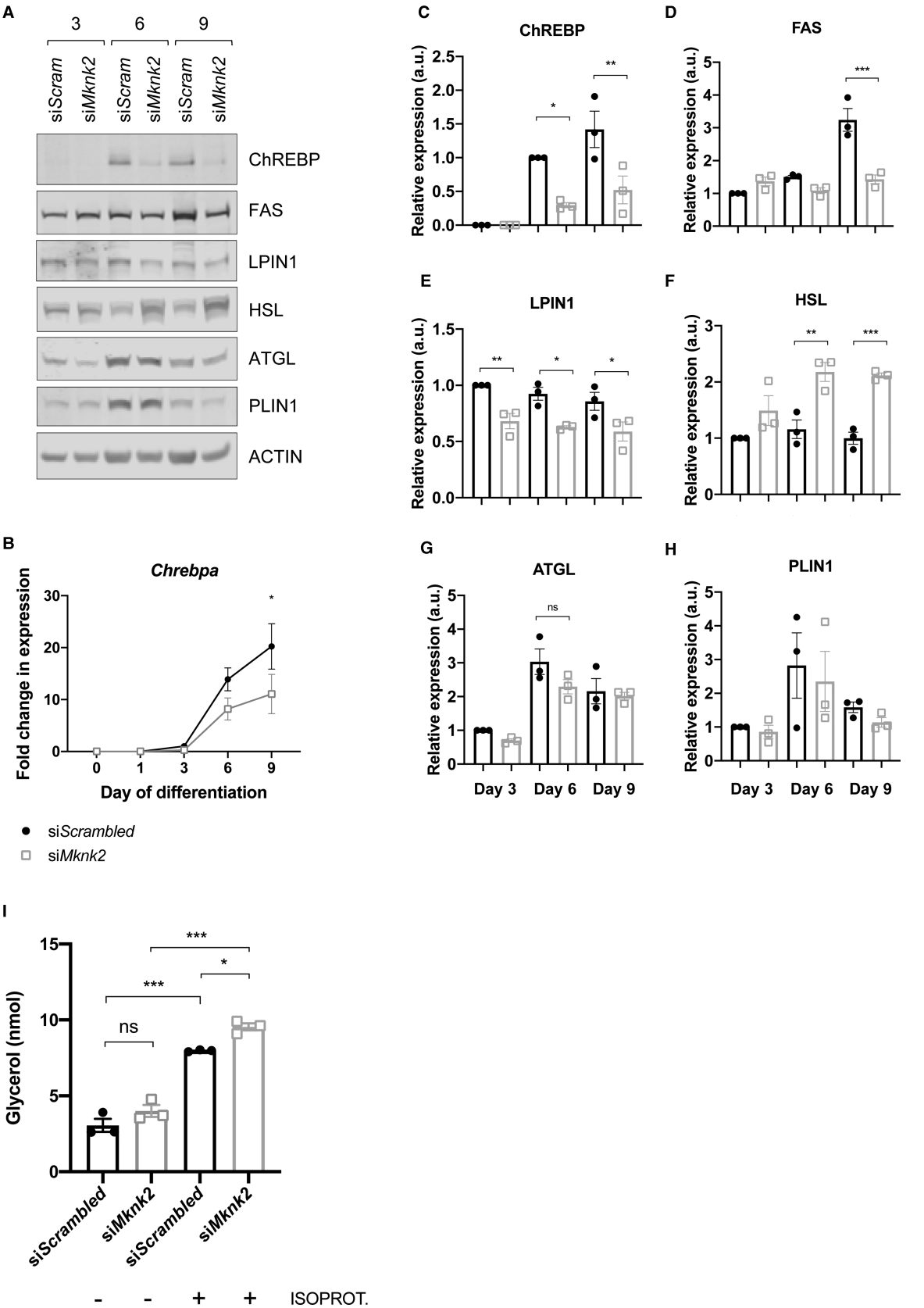

Figure 4. Effect of MNK2 knock-down on the expression of selected proteins and lipolysis in 3T3-L1 adipocytes. Part 1 of 2

3T3-L1 pre-adipocytes were transfected with siRNA as indicated. (**A**) The levels of ChREBP, FAS, LPIN1, HSL, ATG, PLIN1 and

Figure 4. Effect of MNK2 knock-down on the expression of selected proteins and lipolysis in 3T3-L1 adipocytes. Part 2 of 2
ACTIN were monitored by Western blot at the indicated times as quantified in (**C–H**); representative immunoblots are shown ($n = 3$); one-way ANOVA (*$P < 0.05$ **$P < 0.01$ ***$P < 0.001$). (**B**) The mRNA level of *Chrebpa* was measured by RT-qPCR ($n = 3$); 2-way ANOVA (*$P < 0.05$ **$P < 0.01$ ***$P < 0.001$). (**I**) Glycerol levels were measured in medium from day 9 adipocytes treated with or without 100 nM isoproterenol ($n = 3$); one-way ANOVA (*$P < 0.05$ **$P < 0.01$ ***$P < 0.001$).

were significantly decreased by the knock-down of MNK2 on day 9 (Figure 4A,D). This suggests that MNK2 may regulate lipogenic gene expression by regulating the levels of ChREBP. Consistent with these findings, ChREBP depletion in precursor adipocytes has previously been demonstrated to reduce lipid accumulation and partially inhibit adipocyte differentiation [55].

LPIN1 expression was also significantly reduced in MNK2 knock-down adipocytes on days 3, 6 and 9 (Figure 4A,E), despite *Lpin1* mRNA being only significantly reduced on day 6 (Figure 3F). The discrepancy between mRNA and protein levels suggests MNK2 may regulate LPIN1 expression, as mentioned earlier. HSL expression was significantly increased by the knock-down of MNK2 on days 6 and 9 (Figure 4A,F), consistent with *Lipe* mRNA levels (Figure 3H). The level of ATGL was not significantly affected by MNK2 knock-down whilst the abundance of PLIN1, which regulates lipolytic activity at the lipid droplet interface, was unchanged (Figure 4A,G,H), consistent with the lack of a significant change in *Plin1* mRNA levels (Figure 3K).

The increased levels of HSL prompted us to test the rate of lipolysis under basal conditions following stimulation of differentiated 3T3-L1 cells by the adrenergic agonist isoproterenol. As expected, isoproterenol markedly increased the production of glycerol (generated by lipolysis) and this effect was greater in cells where MNK2 was knocked down (Figure 4I). This suggests that knock-down of MNK2 moderately increases the rate of stimulated lipolysis perhaps due to elevated HSL expression. The rate of basal lipolysis was not significantly increased, consistent with the fact that access to the lipid droplet surface is blocked under these conditions by PLIN1 [58].

Because ChREBP is activated by glucose metabolites, its reduced expression could be explained by altered intracellular glucose levels. To assess whether glucose transport was regulated by MNK2, glucose uptake was assayed quantitatively in response to insulin dosage in MNK2 knock-down adipocytes. Unexpectedly, glucose uptake was significantly elevated by the knock-down of MNK2, even under basal conditions (Figure 5A), suggesting that MNK2 may negatively regulate glucose uptake or insulin signalling more broadly. However, the expression of insulin-responsive glucose transporter GLUT4 (*Slc2a4)* at both the mRNA (Figure 3Q) and protein levels (Figure 5B–D) were not statistically different.

The increase in glucose uptake observed in MNK2 knock-down adipocytes was likely to have implications for glycolytic metabolism. Using phenol red as an indicator of the acidity of the medium, the rate of acidification in differentiating adipocytes in which MNK2 was knocked down was greater than in adipocytes with normal MNK2 levels (data not shown). This could reflect faster glycolysis in MNK2 knock-down adipocytes, since increased glycolytic flux would generate more L-lactate and thereby lower the pH of the growth medium more quickly (see scheme in Supplementary Figure S2). In support of this, L-lactate levels were higher in MNK2 knock-down adipocytes suggesting that these cells do indeed exhibit moderately increased glycolytic flux (Figure 5F).

The nuclear translocation of ChREBPα is an important regulatory event that is necessary to induce ChREBPβ and a program of lipogenic and glycolytic gene transcription. The physical interaction of ChREBP with other proteins has been shown to regulate its nuclear translocation: for instance, over-expression of HSL impedes ChREBPα translocation and thereby reduces transcription of lipogenic genes [27]. In si*Mknk2* adipocytes, the reduction in ChREBP was associated with reduced lipogenic gene expression (Figures 2B and 3A–F), increased β-adrenergic stimulated lipolysis (Figure 4I) and consequently, reduced lipid accumulation (Figure 2C–E). Given MNK2, like HSL, is cytoplasmic, it was possible that MNK2 may positively regulate the nuclear translocation of ChREBPα by physical interaction. However, we were consistently unable to detect an interaction between ChREBP and MNK2 (data not shown).

Given the metabolic effects described thus far are a result of siRNA-mediated knock-down of MNK2, it was important to assess whether inhibition of the kinase activity of MNK2 exerted similar effects. To assess this, 3T3-L1 pre-adipocytes were subjected to adipogenic differentiation in the presence or absence of the selective MNK1/2 inhibitor eFT508 [24], and the expression of key metabolic genes was assessed by RT-qPCR.

Biochemical Journal (2020) 477 2735–2754
https://doi.org/10.1042/BCJ20200433

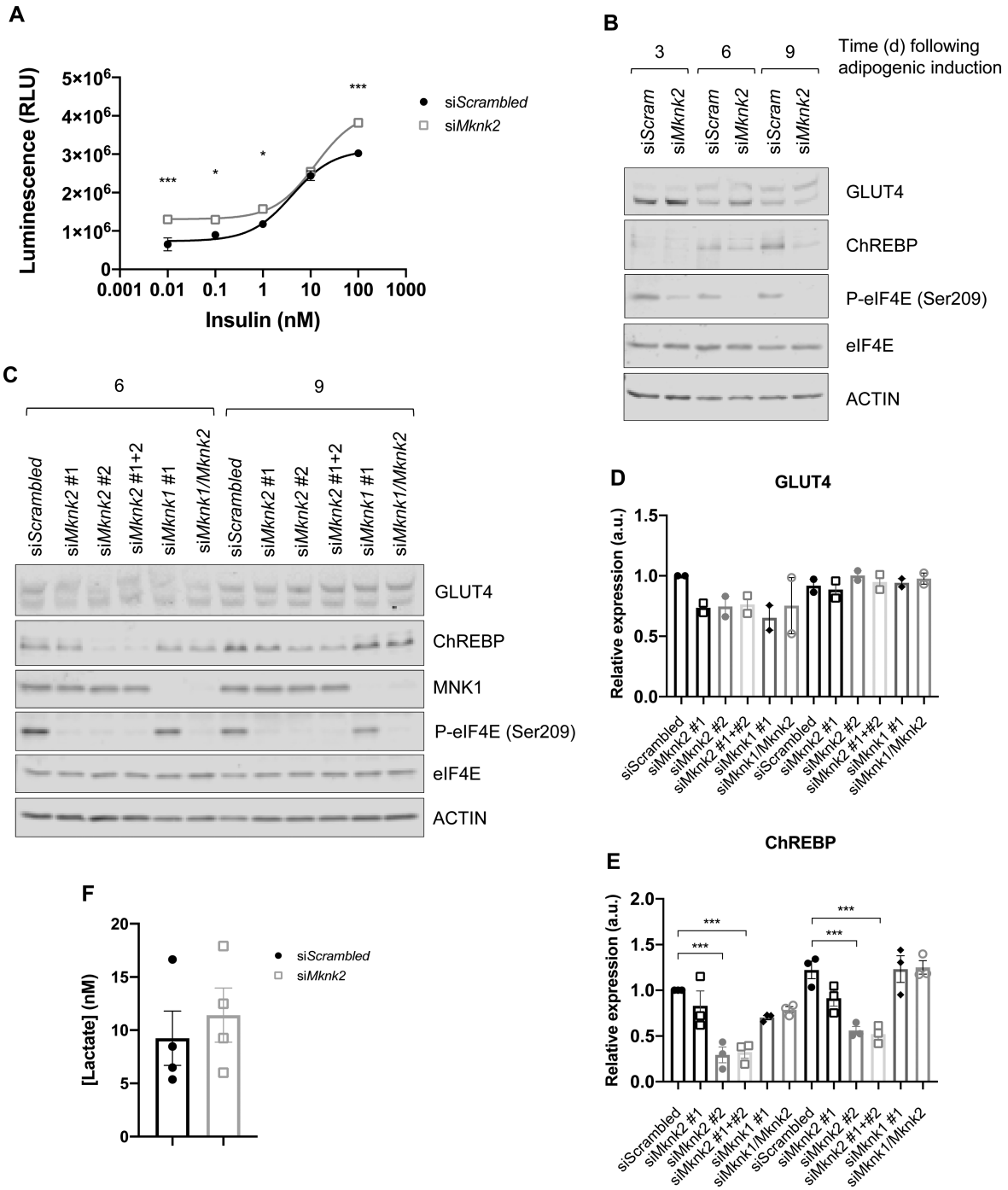

Figure 5. Knock-down of MNK2 affects levels of ChREBP and glucose uptake in 3T3-L1 adipocytes.

3T3-L1 pre-adipocytes were transfected with siRNA individually or in combination, as indicated. (**A**) Glucose uptake in response to insulin was measured in day 9 adipocytes ($n = 3$); 2-way ANOVA (*$P < 0.05$ **$P < 0.01$ ***$P < 0.001$). (**B**,**C**) The levels of GLUT4, ChREBP, p-eIF4E, eIF4E, MNK1 and ACTIN were monitored by Western blot at the indicated times; representative immunoblots are shown ($n = 2$–3). The levels of (**D**) GLUT4 and (**E**) ChREBP were quantified from (**C**). (**F**) L-Lactate levels were measured in the growth medium for day-6 adipocytes ($n = 4$).

To assess the required dose of eFT508, which inhibits MNK1 and MNK2 [24], 3T3-L1 cells were treated with a range of concentrations of this compound, and p-eIF4E was monitored as a readout of MNK activity. eFT508 substantially blocked eIF4E phosphorylation even at 0.01 μM (Supplementary Figure S4). At a

Biochemical Journal (2020) **477** 2735–2754
https://doi.org/10.1042/BCJ20200433

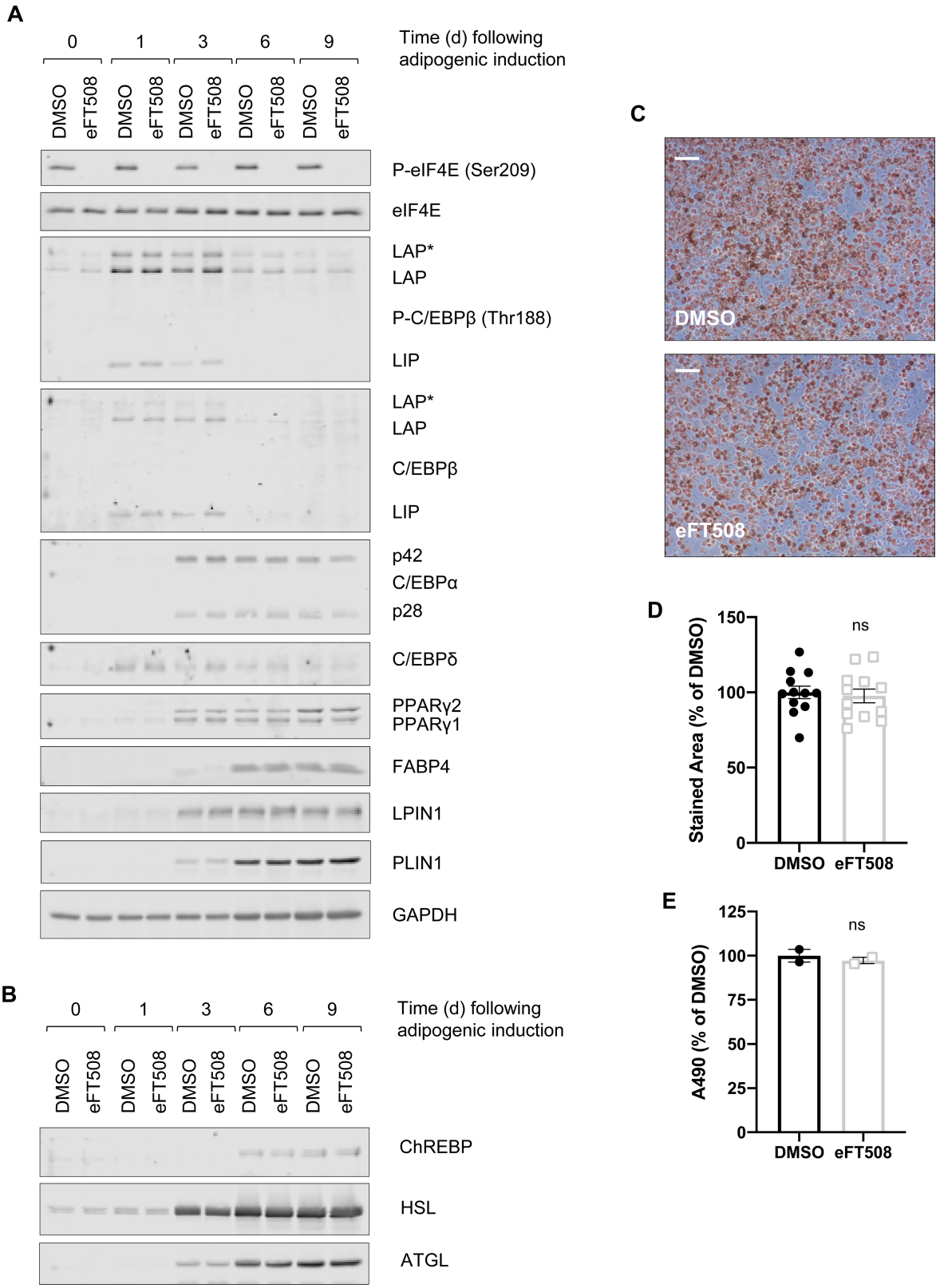

Figure 6. MNK activity does not regulate adipogenesis or triglyceride accumulation in 3T3-L1 cells. Part 1 of 2

3T3-L1 pre-adipocytes were pre-treated with 0.3 μM eFT508 or equivalent volume of DMSO. (**A**,**B**) Protein expression monitored by Western blot using the indicated antibodies; representative immunoblots are shown ($n = 3$). (**C**) Day 9

Biochemical Journal (2020) 477 2735–2754
https://doi.org/10.1042/BCJ20200433

Figure 6. MNK activity does not regulate adipogenesis or triglyceride accumulation in 3T3-L1 cells. Part 2 of 2

differentiated adipocytes were stained with ORO to assess lipid accumulation; representative images are shown, scale bar 0.2 μm. (**D**) Total stained area was quantified from (**C**) or from the absorbance of eluted ORO at 490 nm (**E**); data are mean ± SEM ($n = 3$); unpaired *t*-test (*$P < 0.05$ **$P < 0.01$ ***$P < 0.001$).

concentration of 0.3 μM, eFT508 completely eliminated p-eIF4E and this concentration was selected for further studies. At this concentration, eFT508 did not affect any of the other signalling pathways tested (i.e. phosphorylation of ERK, PKB/Akt, or ribosomal protein S6 or eIF4E binding protein 1, 4E-BP1, both of which lie downstream of mTORC1), except for a minor impairment of ERK or PKB phosphorylation at the highest concentration tested (5 μM, i.e. >15× higher than that used in our studies here).

Importantly, in contrast with the effects of knock-down of MNK2, the levels of *Acaca*, *Acacb*, *Acly*, *Fasn*, *Dgat1*, *Dgat2* and *Sfrp5*, were not significantly reduced by eFT508 (Supplementary Figure S5A–G); in fact, some mRNAs were, at some time-points, marginally or significantly increased. Furthermore, the level of *Lipe* was not significantly increased by eFT508, suggesting that the regulation of HSL expression is independent of the catalytic activity of MNK2 (Supplementary Figure S5L). The levels of key metabolic proteins were assessed in adipocytes differentiated in the presence of eFT508. As expected, and in contrast with the knock-down of MNK2, the expression of FAS, HSL, ATGL, LPIN1 and PLIN1 was not affected by eFT508 (Figures 6A,B and 7A–F). eFT508 also had no effect on the expression of ChREBP protein or mRNA (Figures 6B and 7A,G). Furthermore, eFT508 had no effect on lipid accumulation as assessed by ORO staining (Figure 6C–E) or on basal or isoproterenol-induced lipolysis (glycerol production) (Figure 7H).

eFT508 did not significantly affect *Srebf1*, *Slc2a4* or *Cd36* mRNA levels (Supplementary Figure S5), consistent with the knock-down of MNK2, nor did eFT508 affect the expression of *Mknk1* and *Mknk2*, as expected (Supplementary Figure S5P,Q). *Plin1* levels were significantly increased by eFT508 on day 6, however, this discrepancy was unlikely to have any major physiological effect given that PLIN1 protein levels are more critical for their regulatory function than its mRNA. Therefore, given eFT508 did not elicit the same changes in gene expression as observed in MNK2 knock-down adipocytes, the observed metabolic changes associated with MNK2 knock-down are suggested to be mediated by a non-catalytic function(s) of MNK2.

Concluding comments

These studies were prompted by our striking observation that MNK2-KO mice are substantially protected against the weight gain that is usually induced by consuming a HFD [12]. Those findings suggested that MNK2, the major MNK in AT, might play a role either in the differentiation of adipocytes (adipogenesis) or in AT lipid metabolism.

Using the well-established 3T3-L1 cell model of adipocyte differentiation, we have explored the role of MNK2 in these processes. Our data clearly show that knocking down the expression of MNK2 did not affect adipogenesis as judged by the unaltered expression of markers of this process. However, knock-down of MNK2 did impair the accumulation of lipids (TAGs, derived in this system from DNL), and the expression of genes and enzymes involved in lipid synthesis/storage.

Our data point to lower expression of the transcription factor ChREBP, which drives expression of many genes that encode enzymes needed for DNL, in cells in which MNK2 has been knocked down. Its mRNA levels were also reduced. These data indicate that MNK2 positively modulates the expression of ChREBP, an important regulator of lipogenic genes, and thus lipid accumulation in adipocytes. Knock-down of MNK2 also decreased the levels of Lipin-1, another important regulator of lipid synthesis (via its effects on the transcription factor SREBP, see e.g. [59]).

An unexpected finding of our study is that these effects were not recapitulated by treating 3T3-L1 cells with a potent and specific MNK inhibitor, eFT508. This indicates that the consequences of knocking down MNK2 are not due to loss of its catalytic activity, but rather to loss of the MNK2 protein itself. Presumably, this is because MNK2 engages in, so far unknown, interactions with other proteins to promote lipogenesis. Interestingly, another target for p38 MAP kinase, the protein kinase MK2, also exerts effects that are independent of its catalytic activity [60].

Thus, our findings show that MNK2 plays a role in promoting lipid accumulation, but not adipocyte differentiation, and help to explain our earlier data [25] showing lower fat accumulation in MNK2-KO mice fed a HFD.

Biochemical Journal (2020) **477** 2735–2754
https://doi.org/10.1042/BCJ20200433

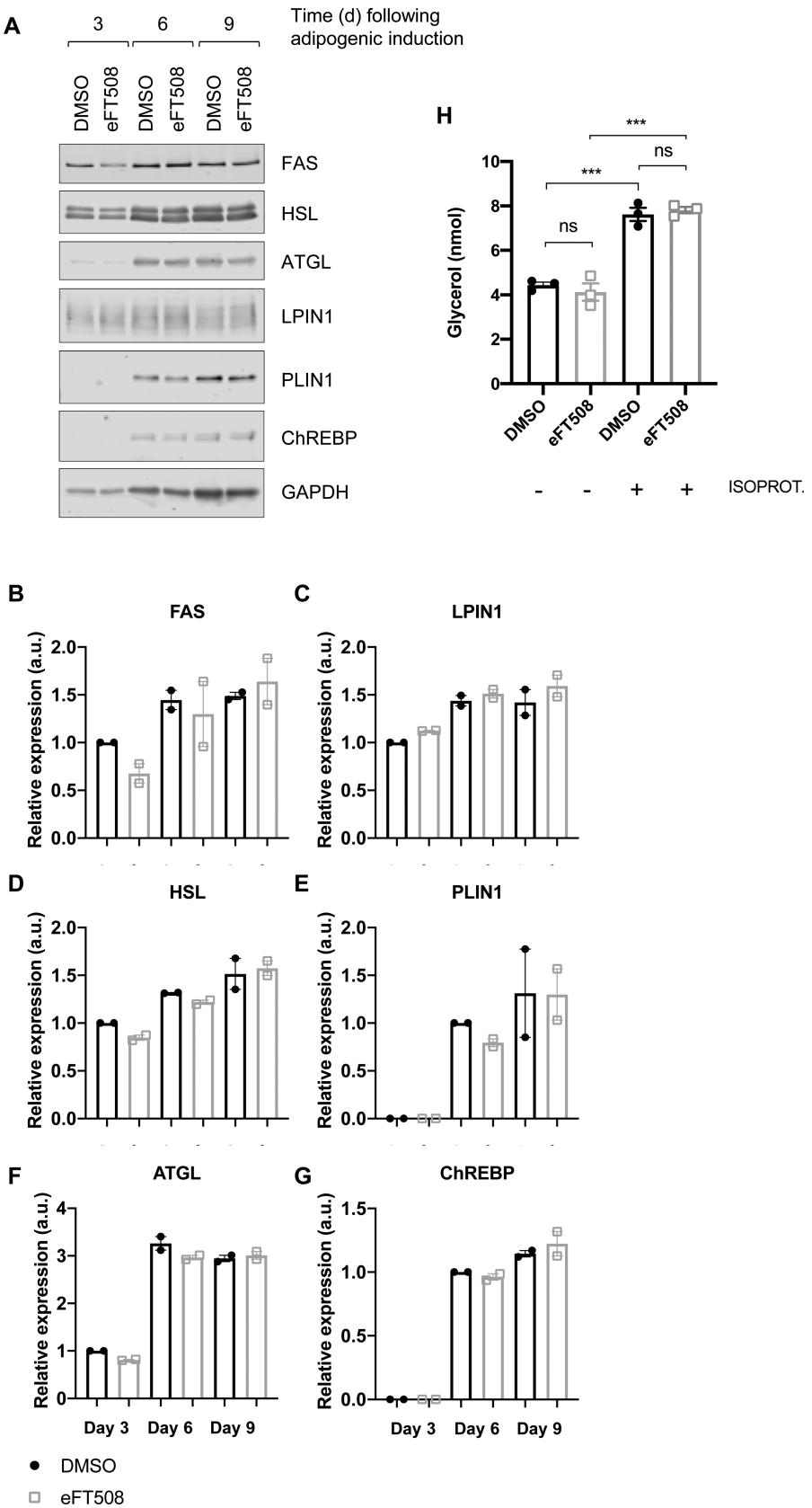

Figure 7. eFT508 does not affect lipolysis or expression of proteins of lipid metabolism in 3T3-L1 cells. Part 1 of 2

3T3-L1 pre-adipocytes were pre-treated with 0.3 μM eFT508 or equivalent volume of DMSO. (**A**) The levels of FAS, HSL, ATGL,

Biochemical Journal (2020) **477** 2735–2754
https://doi.org/10.1042/BCJ20200433

Figure 7. eFT508 does not affect lipolysis or expression of proteins of lipid metabolism in 3T3-L1 cells. Part 2 of 2
LPIN1, PLIN1, ChREBP and GADPH were monitored by Western blot, as quantified in (**B**–**G**). (**H**) Glycerol levels were measured in media from day 9 adipocytes treated with or without 100 nM isoproterenol ($n = 3$); one-way ANOVA (*$P < 0.05$ **$P < 0.01$ ***$P < 0.001$).

Competing Interests
The authors declare that there are no competing interests associated with the manuscript.

Funding
This work was supported by funding from the South Australian Health and Medical Research Institute. JEM acknowledges the support received through the provision of an Australian Government Research Training Program Scholarship. PJP is supported by a L2 Future Leader Fellowship from the National Heart Foundation of Australia [FLF102056] and L2 Career Development Fellowship from the National Health and Medical Research Council [CDF1161506].

Open Access
Open access for this article was enabled by the participation of the University of Adelaide in an all-inclusive *Read & Publish* pilot with Portland Press and the Biochemical Society under a transformative agreement with CAUL.

Author Contributions
J.E.M. and J.X. conducted the experiments; J.E.M. and C.G.P. designed the study; P.J.P. and C.G.P. provided the supervision; C.G.P. obtained the funding.

Acknowledgements
3T3-L1 embryonic fibroblasts were generously provided by Dr. Yeesim Khew-Goodall from the Centre for Cancer Biology (University of South Australia, Adelaide, Australia). We thank the South Australian Health and Medical Research for their support for this work.

Abbreviations
AT, adipose tissue; C/EBP, CCAAT/enhancer-binding protein; DNL, *de novo* lipogenesis; eIF4E, eukaryotic initiation factor 4E; ERK, extracellular regulated kinase; FA, fatty acid; HFD, high-fat diet; MAPK, mitogen-activated protein kinase; MNKs, MAPK-interacting kinases; PPARγ, peroxisome proliferator-activated receptor-γ; SDS–PAGE, sodium-dodecyl sulfate polyacrylamide gel electrophoresis; siRNA, small-interfering RNA; TPA, tetradecanoylphorbol acetate.

References
1 Tang, Q.Q. and Lane, M.D. (2012) Adipogenesis: from stem cell to adipocyte. *Annu. Rev. Biochem.* **81**, 715–736 https://doi.org/10.1146/annurev-biochem-052110-115718
2 Shepherd, P.R., Gnudi, L., Tozzo, E., Yang, H., Leach, F. and Kahn, B.B. (1993) Adipose cell hyperplasia and enhanced glucose disposal in transgenic mice overexpressing GLUT4 selectively in adipose tissue. *J. Biol. Chem.* **268**, 22243–22246 PMID: 8226728
3 Lafontan, M. (2014) Adipose tissue and adipocyte dysregulation. *Diabetes Metab.* **40**, 16–28 https://doi.org/10.1016/j.diabet.2013.08.002
4 Green, H. and Kehinde, O. (1975) An established preadipose cell line and its differentiation in culture. II. factors affecting the adipose conversion. *Cell* **5**, 19–27 https://doi.org/10.1016/0092-8674(75)90087-2
5 MacDougald, O.A. and Lane, M.D. (1995) Transcriptional regulation of gene expression during adipocyte differentiation. *Annu. Rev. Biochem.* **64**, 345–373 https://doi.org/10.1146/annurev.bi.64.070195.002021
6 Green, H. and Kehinde, O. (1976) Spontaneous heritable changes leading to increased adipose conversion in 3T3 cells. *Cell* **7**, 105–113 https://doi.org/10.1016/0092-8674(76)90260-9
7 Green, H. and Meuth, M. (1974) An established pre-adipose cell line and its differentiation in culture. *Cell* **3**, 127–133 https://doi.org/10.1016/0092-8674(74)90116-0
8 Student, A.K., Hsu, R.Y. and Lane, M.D. (1980) Induction of fatty acid synthetase synthesis in differentiating 3T3-L1 preadipocytes. *J. Biol. Chem.* **255**, 4745–4750 PMID: 7372608
9 Coleman, R.A., Reed, B.C., Mackall, J.C., Student, A.K., Lane, M.D. and Bell, R.M. (1978) Selective changes in microsomal enzymes of triacylglycerol phosphatidylcholine, and phosphatidylethanolamine biosynthesis during differentiation of 3T3-L1 preadipocytes. *J. Biol. Chem.* **253**, 7256–7261 PMID: 701249

10 Tontonoz, P. and Spiegelman, B.M. (2008) Fat and beyond: the diverse biology of PPARgamma. *Annu. Rev. Biochem.* **77**, 289–312 https://doi.org/10.1146/annurev.biochem.77.061307.091829
11 Nielsen, R., Pedersen, T.A., Hagenbeek, D., Moulos, P., Siersbaek, R., Megens, E. et al. (2008) Genome-wide profiling of PPARgamma:RXR and RNA polymerase II occupancy reveals temporal activation of distinct metabolic pathways and changes in RXR dimer composition during adipogenesis. *Genes Dev.* **22**, 2953–2967 https://doi.org/10.1101/gad.501108
12 Moore, C.E., Pickford, J., Cagampang, F.R., Stead, R.L., Tian, S., Zhao, X. et al. (2016) MNK1 and MNK2 mediate adverse effects of high-fat feeding in distinct ways. *Sci. Rep.* **6**, 23476 https://doi.org/10.1038/srep23476
13 Merrett, J.E., Psaltis, P.J. and Proud, C.G. (2020) Identification of DNA response elements regulating expression of CCAAT/enhancer-binding protein (C/EBP) β and δ during early adipogenesis. *bioRxiv* https://doi.org/10.1080/21623945.2020.1796361
14 Waskiewicz, A.J., Flynn, A., Proud, C.G. and Cooper, J.A. (1997) Mitogen-activated kinases activate the serine/threonine kinases Mnk1 and Mnk2. *EMBO J.* **16**, 1909–1920 https://doi.org/10.1093/emboj/16.8.1909
15 Fukunaga, R. and Hunter, T. (1997) Mnk1, a new MAP kinase-activated protein kinase, isolated by a novel expression screening method for identifying protein kinase substrates. *EMBO J.* **16**, 1921–1933 https://doi.org/10.1093/emboj/16.8.1921
16 Buxade, M., Parra-Palau, J.L. and Proud, C.G. (2008) The mnks: MAP kinase-interacting kinases (MAP kinase signal-integrating kinases). *Front. Biosci.* **13**, 5359–5373 https://doi.org/10.2741/3086
17 Waskiewicz, A.J., Johnson, J.C., Penn, B., Mahalingam, M., Kimball, S.R. and Cooper, J.A. (1999) Phosphorylation of the cap-binding protein eukaryotic translation factor 4E by protein kinase Mnk1 *in vivo*. *Mol. Cell. Biol.* **19**, 1871–1880 https://doi.org/10.1128/MCB.19.3.1871
18 Wang, X., Flynn, A., Waskiewicz, A.J., Webb, B.L., Vries, R.G, Baines, I.A. et al. (1998) The phosphorylation of eukaryotic initiation factor eIF4E in response to phorbol esters, cell stresses and cytokines is mediated by distinct MAP kinase pathways. *J. Biol. Chem.* **273**, 9373–9377 https://doi.org/10.1074/jbc.273.16.9373
19 Goto, S., Yao, Z. and Proud, C.G. (2009) The C-terminal domain of Mnk1a plays a dual role in tightly regulating its activity. *Biochem. J.* **423**, 279–290 https://doi.org/10.1042/BJ20090228
20 Scheper, G.C., Morrice, N.A., Kleijn, M. and Proud, C.G. (2001) The MAP kinase signal-integrating kinase Mnk2 is an eIF4E kinase with high basal activity in mammalian cells. *Mol. Cell. Biol.* **21**, 743–754 https://doi.org/10.1128/MCB.21.3.743-754.2001
21 Scheper, G.C., Parra, J.-L., Wilson, M.L., van Kollenburg, B., Vertegaal, A.C.O., Han, Z.-G. et al. (2003) The N and C termini of the splice variants of the human mitogen-activated protein kinase-interacting kinase Mnk2 determine activity and localization. *Mol. Cell. Biol.* **23**, 5692–5705 https://doi.org/10.1128/MCB.23.16.5692-5705.2003
22 Ueda, T., Watanabe-Fukunaga, R., Fukuyama, H., Nagata, S. and Fukunaga, R. (2004) Mnk2 and Mnk1 are essential for constitutive and inducible phosphorylation of eukaryotic initiation factor 4E but not for cell growth or development. *Mol. Cell. Biol.* **24**, 6539–6549 https://doi.org/10.1128/MCB.24.15.6539-6549.2004
23 Flynn, A. and Proud, C.G. (1995) Serine 209, not serine 53, is the major site of phosphorylation in initiation factor eIF-4E in serum-treated Chinese hamster ovary cells. *J. Biol. Chem.* **270**, 21684–21688 https://doi.org/10.1074/jbc.270.37.21684
24 Reich, S.H., Sprengeler, P.A., Chiang, G.G., Appleman, J.R., Chen, J., Clarine, J. et al. (2018) Structure-based design of pyridone-Aminal eFT508 targeting dysregulated translation by selective mitogen-activated protein kinase interacting kinases 1 and 2 (MNK1/2) inhibition. *J. Med. Chem.* **61**, 3516–3540 https://doi.org/10.1021/acs.jmedchem.7b01795
25 Liu, R., Iadevaia, V., Averous, J., Taylor, P.M., Zhang, Z. and Proud, C.G. (2014) Impairing the production of ribosomal RNA activates mammalian target of rapamycin complex 1 signalling and downstream translation factors. *Nucleic Acids Res.* **42**, 5083–5096 https://doi.org/10.1093/nar/gku130
26 Xie, J., Shen, K., Jones, A.T., Yang, J., Tee, A.R., Shen, M.H. et al. (2020) Reciprocal signaling between mTORC1 and MNK2 controls cell growth and oncogenesis. *Cell. Mol. Life Sci.* https://doi.org/10.1007/s00018-020-03491-1
27 Morigny, P., Houssier, M., Mairal, A., Ghilain, C., Mouisel, E., Benhamed, F. et al. (2019) Interaction between hormone-sensitive lipase and ChREBP in fat cells controls insulin sensitivity. *Nat. Metab.* **1**, 133–146 https://doi.org/10.1038/s42255-018-0007-6
28 Peterfy, M., Phan, J., Xu, P. and Reue, K. (2001) Lipodystrophy in the fld mouse results from mutation of a new gene encoding a nuclear protein, lipin. *Nat. Genet.* **27**, 121–124 https://doi.org/10.1038/83685
29 Phan, J., Peterfy, M. and Reue, K. (2004) Lipin expression preceding peroxisome proliferator-activated receptor-gamma is critical for adipogenesis in vivo and in vitro. *J. Biol. Chem.* **279**, 29558–29564 https://doi.org/10.1074/jbc.M403506200
30 Han, G.S. and Carman, G.M. (2010) Characterization of the human LPIN1-encoded phosphatidate phosphatase isoforms. *J. Biol. Chem.* **285**, 14628–14638 https://doi.org/10.1074/jbc.M110.117747
31 Donkor, J., Sariahmetoglu, M., Dewald, J., Brindley, D.N. and Reue, K. (2007) Three mammalian lipins act as phosphatidate phosphatases with distinct tissue expression patterns. *J. Biol. Chem.* **282**, 3450–3457 https://doi.org/10.1074/jbc.M610745200
32 Peterfy, M., Phan, J. and Reue, K. (2005) Alternatively spliced lipin isoforms exhibit distinct expression pattern, subcellular localization, and role in adipogenesis. *J. Biol. Chem.* **280**, 32883–32889 https://doi.org/10.1074/jbc.M503885200
33 Wang, H., Airola, M.V. and Reue, K. (2017) How lipid droplets "TAG" along: Glycerolipid synthetic enzymes and lipid storage. *Biochim. Biophys. Acta Mol. Cell Biol. Lipids* **1862**, 1131–1145 https://doi.org/10.1016/j.bbalip.2017.06.010
34 Liu, Q., Siloto, R.M., Lehner, R., Stone, S.J. and Weselake, R.J. (2012) Acyl-CoA:diacylglycerol acyltransferase: molecular biology, biochemistry and biotechnology. *Prog. Lipid Res.* **51**, 350–377 https://doi.org/10.1016/j.plipres.2012.06.001
35 Cao, H. (2018) Identification of the major diacylglycerol acyltransferase mRNA in mouse adipocytes and macrophages. *BMC Biochem.* **19**, 11 https://doi.org/10.1186/s12858-018-0103-y
36 Castle, J.C., Hara, Y., Raymond, C.K., Garrett-Engele, P., Ohwaki, K., Kan, Z. et al. (2009) ACC2 is expressed at high levels in human white adipose and has an isoform with a novel N-terminus [corrected]. *PLoS One* **4**, e4369 https://doi.org/10.1371/journal.pone.0004369
37 Abu-Elheiga, L., Brinkley, W.R., Zhong, L., Chirala, S.S., Woldegiorgis, G., and Wakil, S.J. (2000) The subcellular localization of acetyl-CoA carboxylase 2. *Proc. Natl. Acad. Sci. U.S.A.* **97**, 1444–1449 https://doi.org/10.1073/pnas.97.4.1444
38 Abu-Elheiga, L., Oh, W., Kordari, P., and Wakil, S.J. (2003) Acetyl-CoA carboxylase 2 mutant mice are protected against obesity and diabetes induced by high-fat/high-carbohydrate diets. *Proc. Natl. Acad. Sci. U.S.A.* **100**, 10207–10212 https://doi.org/10.1073/pnas.1733877100

Biochemical Journal (2020) **477** 2735–2754
https://doi.org/10.1042/BCJ20200433

39 Kimmel, A.R. and Sztalryd, C. (2016) The perilipins: Major cytosolic lipid droplet-Associated proteins and their roles in cellular lipid storage, mobilization, and systemic homeostasis. *Annu. Rev. Nutr.* **36**, 471–509 https://doi.org/10.1146/annurev-nutr-071813-105410

40 Chang, C.L. (2019) Lipoprotein lipase: new roles for an 'old' enzyme. *Curr. Opin. Clin. Nutr. Metab. Care* **22**, 111–115 https://doi.org/10.1097/MCO.0000000000000536

41 Ibrahimi, A. and Abumrad, N.A. (2002) Role of CD36 in membrane transport of long-chain fatty acids. *Curr. Opin. Clin. Nutr. Metab. Care* **5**, 139–145 https://doi.org/10.1097/00075197-200203000-00004

42 Reshef, L., Olswang, Y., Cassuto, H., Blum, B., Croniger, C.M., Kalhan, S.C. et al. (2003) Glyceroneogenesis and the triglyceride/fatty acid cycle. *J. Biol. Chem.* **278**, 30413–30416 https://doi.org/10.1074/jbc.R300017200

43 Forest, C., Tordjman, J., Glorian, M., Duplus, E., Chauvet, G., Quette, J. et al. (2003) Fatty acid recycling in adipocytes: a role for glyceroneogenesis and phosphoenolpyruvate carboxykinase. *Biochem. Soc. Trans.* **31**, 1125–1129 https://doi.org/10.1042/bst0311125

44 Ballard, F.J., Hanson, R.W. and Leveille, G.A. (1967) Phosphoenolpyruvate carboxykinase and the synthesis of glyceride-glycerol from pyruvate in adipose tissue. *J. Biol. Chem.* **242**, 2746–2750 PMID: 6027245

45 Christodoulides, C., Lagathu, C., Sethi, J.K. and Vidal-Puig, A. (2009) Adipogenesis and WNT signalling. *Trends Endocrinol. Metab.* **20**, 16–24 https://doi.org/10.1016/j.tem.2008.09.002

46 Koza, R.A., Nikonova, L., Hogan, J., Rim, J.S., Mendoza, T., Faulk, C. et al. (2006) Changes in gene expression foreshadow diet-induced obesity in genetically identical mice. *PLoS Genet.* **2**, e81 https://doi.org/10.1371/journal.pgen.0020081

47 Lagathu, C., Christodoulides, C., Virtue, S., Cawthorn, W.P., Franzin, C., Kimber, W.A. et al. (2009) Dact1, a nutritionally regulated preadipocyte gene, controls adipogenesis by coordinating the Wnt/beta-catenin signaling network. *Diabetes* **58**, 609–619 https://doi.org/10.2337/db08-1180

48 Okada, Y., Sakaue, H., Nagare, T. and Kasuga, M. (2009) Diet-induced up-regulation of gene expression in adipocytes without changes in DNA methylation. *Kobe J. Med. Sci.* **54**, E241–E249 PMID: 19628964

49 Ouchi, N., Higuchi, A., Ohashi, K., Oshima, Y., Gokce, N., Shibata, R. et al. (2010) Sfrp5 is an anti-inflammatory adipokine that modulates metabolic dysfunction in obesity. *Science* **329**, 454–457 https://doi.org/10.1126/science.1188280

50 Kim, J.B., Wright, H.M., Wright, M., and Spiegelman, B.M. (1998) ADD1/SREBP1 activates PPARgamma through the production of endogenous ligand. *Proc. Natl. Acad. Sci. U.S.A.* **95**, 4333–4337 https://doi.org/10.1073/pnas.95.8.4333

51 Kim, J.B. and Spiegelman, B.M. (1996) ADD1/SREBP1 promotes adipocyte differentiation and gene expression linked to fatty acid metabolism. *Genes Dev.* **10**, 1096–1107 https://doi.org/10.1101/gad.10.9.1096

52 Abdul-Wahed, A., Guilmeau, S. and Postic, C. (2017) Sweet sixteenth for ChREBP: Established roles and future goals. *Cell Metab.* **26**, 324–341 https://doi.org/10.1016/j.cmet.2017.07.004

53 He, Z., Jiang, T., Wang, Z., Levi, M. and Li, J. (2004) Modulation of carbohydrate response element-binding protein gene expression in 3T3-L1 adipocytes and rat adipose tissue. *Am. J. Physiol. Endocrinol. Metab.* **287**, E424–E430 https://doi.org/10.1152/ajpendo.00568.2003

54 Hurtado del Pozo, C., Vesperinas-Garcia, G., Rubio, M.A., Corripio-Sanchez, R., Torres-Garcia, A.J., Obregon, M.J. et al. (2011) ChREBP expression in the liver, adipose tissue and differentiated preadipocytes in human obesity. *Biochim. Biophys. Acta* **1811**, 1194–1200 https://doi.org/10.1016/j.bbalip.2011.07.016

55 Witte, N., Muenzner, M., Rietscher, J., Knauer, M., Heidenreich, S., Nuotio-Antar, A.M. et al. (2015) The glucose sensor ChREBP links De novo lipogenesis to PPARgamma activity and adipocyte differentiation. *Endocrinology* **156**, 4008–4019 https://doi.org/10.1210/EN.2015-1209

56 Sae-Lee, C., Moolsuwan, K., Chan, L. and Poungvarin, N. (2016) ChREBP regulates itself and metabolic genes implicated in lipid accumulation in beta-Cell line. *PLoS One* **11**, e0147411 https://doi.org/10.1371/journal.pone.0147411

57 Poungvarin, N., Chang, B., Imamura, M., Chen, J., Moolsuwan, K., Sae-Lee, C. et al. (2015) Genome-Wide analysis of ChREBP binding sites on male mouse liver and white adipose chromatin. *Endocrinology* **156**, 1982–1994 https://doi.org/10.1210/en.2014-1666

58 Souza, S.C., de Vargas, L.M., Yamamoto, M.T., Lien, P., Franciosa, M.D., Moss, L.G. et al. (1998) Overexpression of perilipin A and B blocks the ability of tumor necrosis factor alpha to increase lipolysis in 3T3-L1 adipocytes. *J. Biol. Chem.* **273**, 24665–24669 https://doi.org/10.1074/jbc.273.38.24665

59 Peterson, T.R., Sengupta, S.S., Harris, T.E., Carmack, A.E., Kang, S.A., Balderas, E. et al. (2011) mTOR complex 1 regulates lipin 1 localization to control the SREBP pathway. *Cell* **146**, 408–420 https://doi.org/10.1016/j.cell.2011.06.034

60 Kotlyarov, A., Yannoni, Y., Fritz, S., Laass, K., Telliez, J.B., Pitman, D. et al. (2002) Distinct cellular functions of MK2. *Mol. Cell. Biol.* **22**, 4827–4835 https://doi.org/10.1128/MCB.22.13.4827-4835.2002